

2023

Section: Earth science

CHARACTERIZATION, AND POTENTIAL OF SUBSURFACE PHOSPHORITE BEARING URANIUM AT EAST MAHAMEID REGION, EGYPT

Mohamed G. Mansour

Misr phosphate Company, Sibaiya, Egypt

Mohamed W. Abd El-Moghny

Department of Geology, Faculty of Science, Al-Azhar University, Egypt, Cairo, Nasr City, m_wageeh@azhar.edu.eg

Ibrahim H. Zidan

Nuclear Materials Authority, 530 Maadi, Cairo, Egypt

Mahmoud M. Hassaan

Department of Geology, Faculty of Science, Al-Azhar University, Egypt, Cairo, Nasr City

Follow this and additional works at: <https://absb.researchcommons.org/journal>

How to Cite This Article

Mansour, Mohamed G.; El-Moghny, Mohamed W. Abd; Zidan, Ibrahim H.; and Hassaan, Mahmoud M. (2023) "CHARACTERIZATION, AND POTENTIAL OF SUBSURFACE PHOSPHORITE BEARING URANIUM AT EAST MAHAMEID REGION, EGYPT," *Al-Azhar Bulletin of Science*: Vol. 34: Iss. 2, Article 5. DOI: <https://doi.org/10.58675/2636-3305.1644>

This Original Article is brought to you for free and open access by Al-Azhar Bulletin of Science. It has been accepted for inclusion in Al-Azhar Bulletin of Science by an authorized editor of Al-Azhar Bulletin of Science. For more information, please contact kh_Mekheimer@azhar.edu.eg.

Characterization, and Potential of Subsurface Phosphorite Bearing Uranium at East Mahameid Region, Egypt

Mohamed G. Mansour^a, Mohamed W. Abd El-Moghny^{b,*}, Ibrahim H. Zidan^c,
Mahmoud M. Hassaan^b

^a Misr Phosphate Company, Sibaiya, Egypt

^b Department of Geology, Faculty of Science, Al-Azhar University, Nasr City, Cairo, Egypt

^c Nuclear Materials Authority, 530 Maadi, Cairo, Egypt

Abstract

The present study deals with geological, mineralogical and geochemical studies of the Upper Cretaceous Duwi Formation bearing phosphorites and its radioactivity at east Mahameid area, Nile Valley, Egypt. In the studied area, 100 boreholes were drilled in three sectors; Abu Sabona (A); Araby (B); and El- Mallaha (C). The selected core samples have been described to illustrate the stratigraphic succession of the investigated area. Thirty phosphorite samples were studied petrographically and analyzed chemically. The chemical analyses were carried out at the Labs of Nuclear Materials Authority (NMA). The obtained data revealed the formation of the Lower Phosphorite Member as isolated lenticular bodies. The Lower Phosphorites Member is deposited in shallower epicontinental marine environment than the upper one. The abnormal concentration of Cr, Ni favor their ultramafic –mafic source rock. The slight difference in cU and eU with increasing in cU contents in most samples relative to eU, could be connected to recent uranium migration from the upper black shale of the Dakhla Formation.

Keywords: Duwi, Egypt, Nile valley, Phosphorite, Uranium

1. Introduction

Due to its economic interest, the Upper Campanian, phosphate-rich, Duwi Formation has been intensely studied. The increased interest in these phosphorite deposits of the Duwi Formation coincides with the discoveries of oil shale and rare earth elements associated with the phosphate deposits [1]. The Duwi Formation was studied by several authors who described their stratigraphy, petrography, geochemistry and phosphogenesis [2–11]. The phosphorites of the studied Duwi Formation are mined at three major regions on the Red Sea coastal zone (e.g. Safaga–Qusseir district), on both banks of the Nile Valley (e.g. Sibaiya and Mahameid), and Western Desert (e.g. Abu Tartur plateau and Dakhla Oasis). The phosphorite

reserves in these localities are not clearly calculated. However, the estimated geological reserves are more than about 70 million tons at Nile Valley [12].

Upper Campanian phosphate deposits in Egypt occur in basins that remained relatively tectonically undeformed representing stable shelf areas [11]. In contrast, the Duwi area, at the northwestern margin of the Red Sea, can be considered as tilted faulted blocks that are generally dissected by minor faults, especially in the northern and southern parts [13]. A major phosphogenic episode took place during the late Campanian in the North Africa [14] that was a part of the broad, shallow, southern epicontinental shelf of the Tethys Ocean, situated between 10° and 20° N palaeo-latitudes [15]. The prevailing winds were blowing to the west and southwest onto the southern Neo-Tethys epicontinental shelf creating

Received 13 December 2022; revised 21 January 2023; accepted 26 January 2023.
Available online 8 September 2023

* Corresponding author. 11884, Nasr City, Cairo, Egypt. Fax. +2 0222629353.
E-mail address: sm_wageeh@azhar.edu.eg (M.W. Abd El-Moghny).

<https://doi.org/10.21608/2636-3305.1644>

2636-3305/© 2023, The Authors. Published by Al-Azhar university, Faculty of science. This is an open access article under the CC BY-NC-ND 4.0 Licence (<https://creativecommons.org/licenses/by-nc-nd/4.0/>).

an upwelling regime from the deeper Neo-Tethys Ocean onto this shelf [14,16]. The depositional setting caused rapid lateral variations in thickness and facies. The Egyptian phosphates are shallow marine deposits. The maximum phase of phosphorite sedimentation was associated with a transgressive shoreline of the Neo-Tethys Ocean that encroached from north to south over the northern margin of Africa during Coniacian to Campanian times [17].

The aim of the present study is to present the results of an investigation of the lithofacies, mineralogy and geochemistry of the studied bearing Cretaceous rocks to determine their petrographical and geochemical characteristics and its radioactivity in some subsurface sections, East Mahameid area, Nile Valley. The study area is located between longitudes 32° and 32° 47' 00 E– and latitudes 25° 9' and 25° 11' N along the right bank of the Nile Valley (Fig. 1).

2. Methods of study

In the present work, 100 boreholes have been drilled and the lithostratigraphic sections of the Duwi Formation, cover all the studied area (Fig. 2), have been measured in the field and sampled. Thirty phosphorite sample were collected and

described from the drilled boreholes. The thin sections of these phosphorite samples have been studied using polarizing microscope to identify their mineral constituents and petrographical textures. Besides, 10 selected phosphatic samples have been studied by XRD technique, using PHILIPS PW 3710/31 diffractometer, scintillation counter; Cu-target tube and Ni filter at 40 kV and 30 mA, to identify the semi-quantitative distribution of the different minerals in these studied phosphorites.

The major oxides in the phosphatic samples have been calculated by using the conventional wet chemical methods. SiO₂, TiO₂, Al₂O₃ and P₂O₅ contents are determined using the spectrophotometric method, Na₂O and K₂O contents are analyzed by the flame photometric method, Fe₂O₃, MgO and CaO by mean of EDTA complex method as volumetrically technique and loss on ignition, (L.O.I.) by heating at 1000 °C after drying at 110 °C. The content of the trace elements has been determined using the XRF technique. The uranium and thorium concentrations were determined by multi-channel analyzer gamma ray spectrometer. The uranium content is chemically determined by LABOMED spectrophotometric coulometrically using Arenaso III method. All the analyses were carried out in the laboratories of the Egyptian Nuclear Materials Authority (NMA).

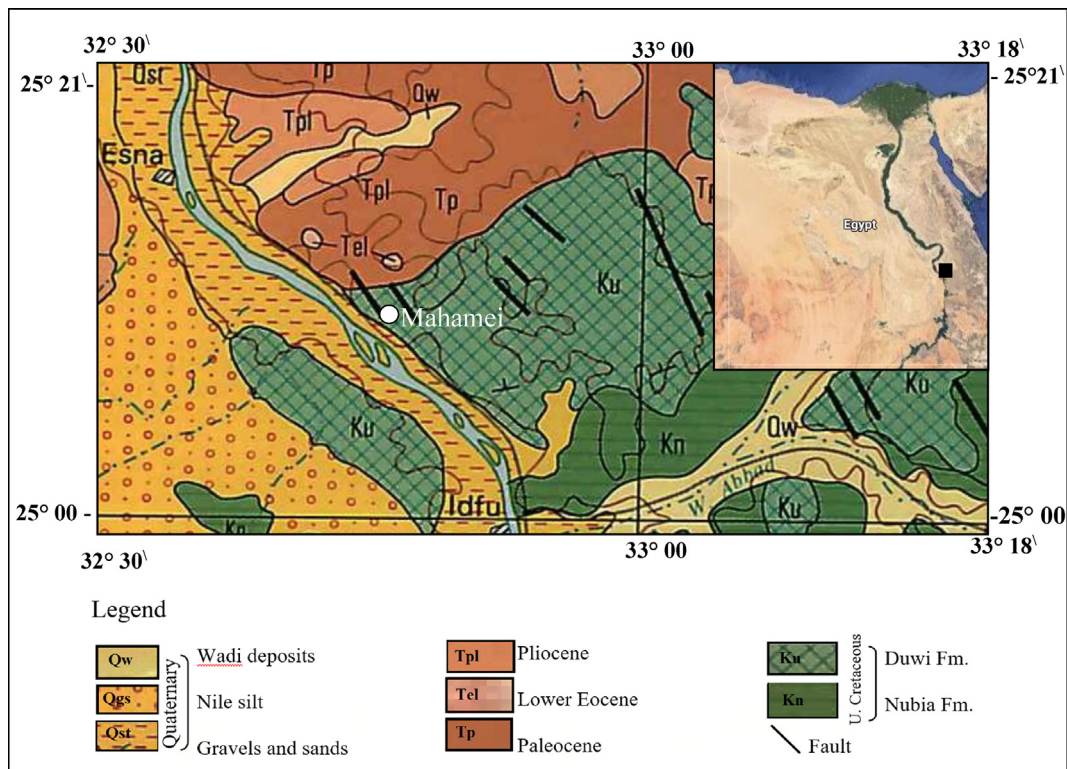


Fig. 1. Geologic map of the studied area (modified after Geological Survey of Egypt, 1981).

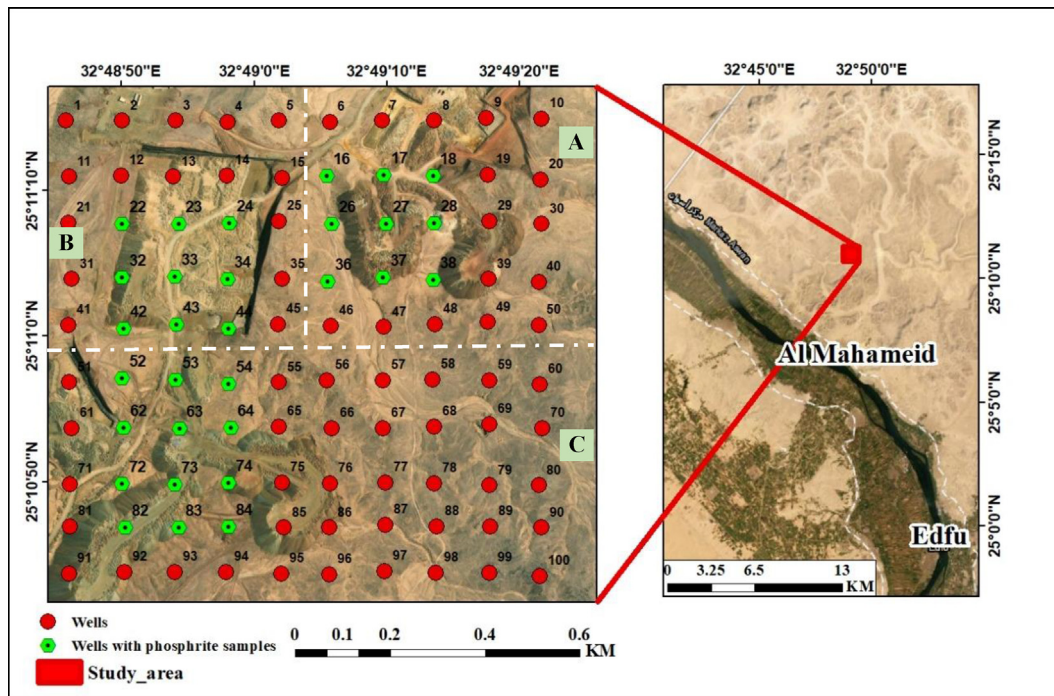


Fig. 2. The distribution of the drilled boreholes in the studied East Mahameid area.

3. Lithostratigraphy

Several stratigraphical studies were carried out on the Esna – Idfu district [2,18,19] to classify the Upper Cretaceous-Lower Eocene succession in the Nile Valley region. In the studied area, the basal part of this sequence is the Nubia Formation (Taref Sandstone and Qusseir Variegated Shale), conformably overlain by the Duwi, and Dakhla formations. The term ‘Duwi Formation’ was introduced to describe the Upper Cretaceous phosphate bearing rock unit at Gebel Duwi [20]. The studied Duwi Formation is conformably overlain by the Dakhla Formation (Fig. 3), that is made up of black fissile shale with thin intercalated beds of silty clay. The maximum thickness of the Dakhla Formation in the studied area (10 m) can be measured at the northern part relative to 1 m at the southern part.

The sections of the Duwi Formation are exposed by open pit mining and revealed that this rock unit is fossiliferous including some ammonites and other molluscan faunas in addition to some shark teeth. These faunas attributed the Duwi Formation to the Campanian [18,21–23]. The Campanian – Maastrichtian is considered the age of this formation by [13,24–30], while [13,27–29] of Lower Maastrichtian age. However [11], studied the calcareous nanofossils at Gebel Duwi section introducing the Upper Campanian age for the Duwi Formation.

In the studied area, the Duwi Formation is composed of oxidized, yellow to brownish

phosphorite, intercalated with thin black shale, dolomitic lenses and oyster limestone beds (Fig. 3). This formation ranges in thickness from 1 up to 10 m and attains its maximum thickness in the north-western part of the studied area (site B).

In some drilled wells the rocks of the Duwi Formation are not recorded, where the total drilled succession is represented only by shales of the Dakhla Formation (Fig. 3). The deposition of the Lower Member of the Duwi formation in the studied area probably controlled by the paleogeographic features of the basin. The isolith contour map of the total thickness of the studied phosphorites matches relatively with the increase of the thickness of the Duwi Formation (Fig. 5).

The Duwi Formation in the studied area comprises three informal members; lower, middle and upper members. The Lower Member, the basal unit, is composed of yellowish brown phosphate beds interbedded with thin black shale bands, lenses of dolomite, chert and oyster phosphatic limestone (Fig. 6). The thickness of this member ranges from 6 to 7 m thick and attains a maximum thickness (7 m) in the central part of the studied area (Fig. 3). The isopach map of the drilled Lower Member revealed that this member form as slightly isolated lenticular bodies (apparently bedded) with maximum thickness at troughs (Fig. 4). This phenomenon associated with synclines [30,31].

The Middle Member is composed of grey to black, papery shale and its thickness ranges from 4 to

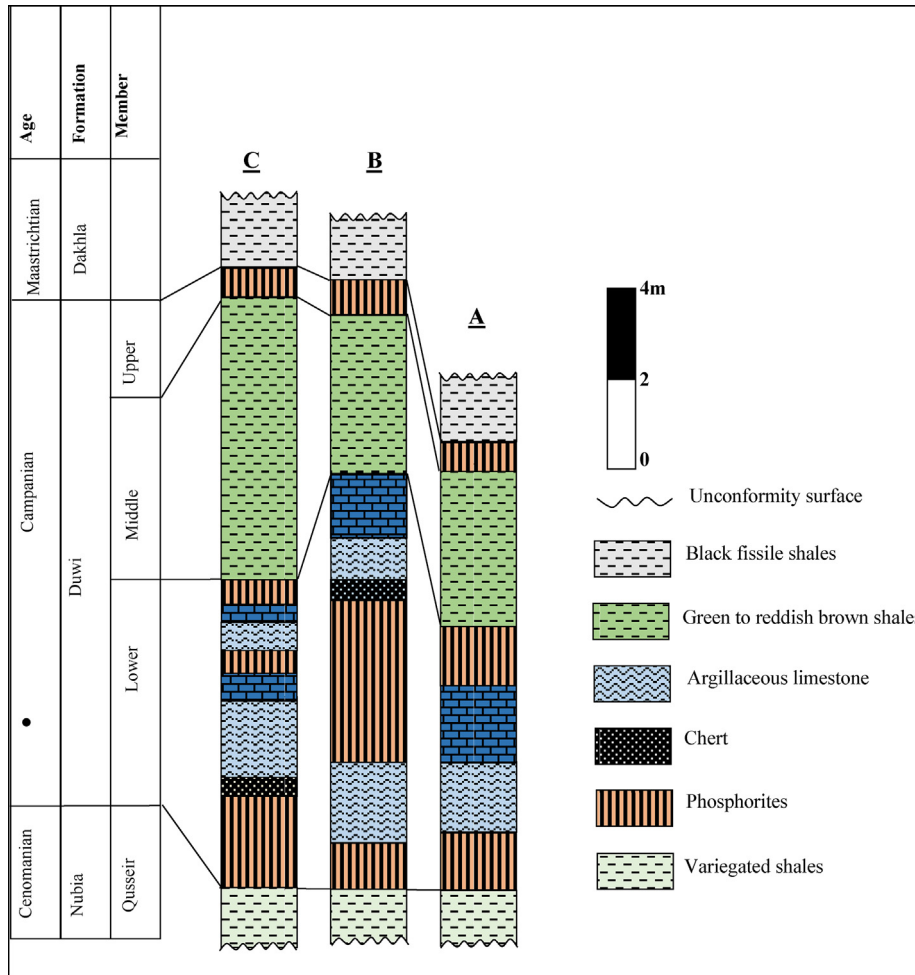


Fig. 3. Stratigraphic sequence with maximum thickness of the drilled boreholes in studied sectors: A) Abu Sabuna; B) Araby; and C) EL-Mallaha, at East Mahameid area.

7.5 m, where its maximum thickness is measured in the central part of the study area.

The Upper Member is the uppermost unit of the Duwi Formation and composed of yellowish

brown phosphorites. The upper member ranges in thickness from 15 to 30 cm and its maximum thickness is recorded in the northern part of the study area.

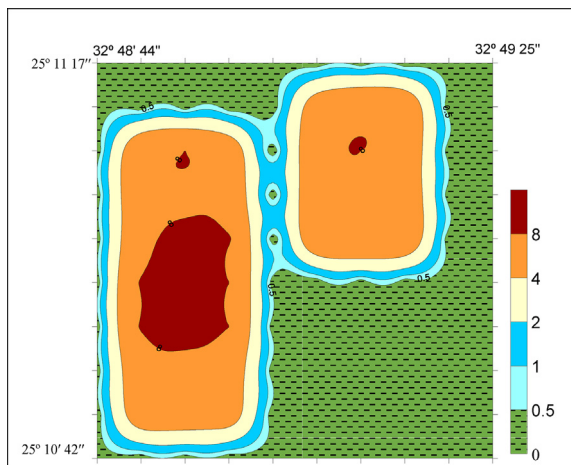


Fig. 4. Isoline map of the total thickness of the Lower Member of the Duwi Formation in the drilled boreholes at East Mahameid area.

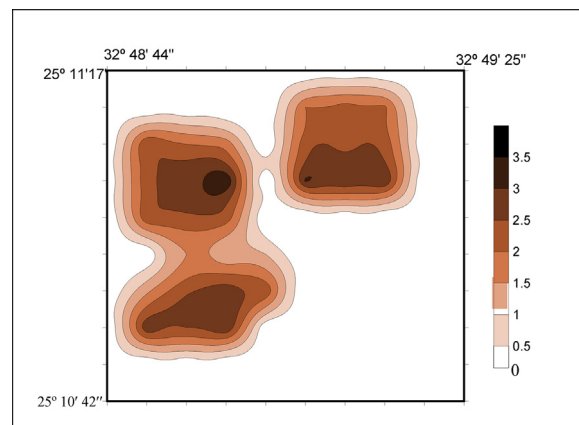


Fig. 5. Isolith map shows the distribution of the phosphorite thickness of the Duwi Formation in east Mahameid area.

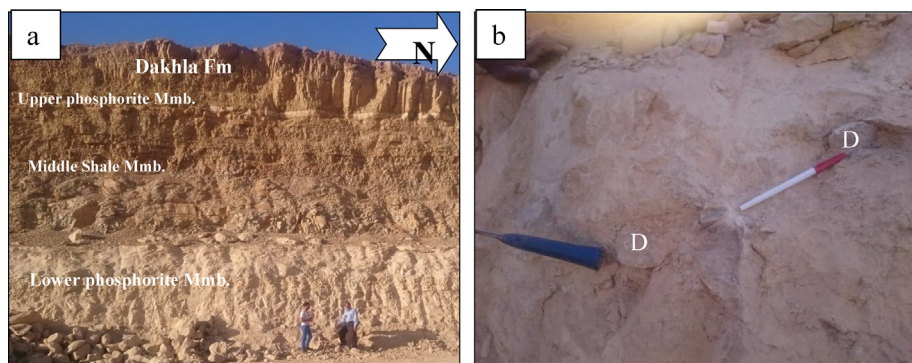


Fig. 6. Field photograph showing the exposed stratigraphic section of the studied area: (a) three members of the Duwi Formation that overlain by the Dakhla Formation; (b) dolomitic lenses (D) intercalated within phosphatic beds.

4. Results and discussion

4.1. Petrographic features

Microscopically, the different components of the studied phosphate samples can be conveniently grouped into three principal components namely: phosphate particles, non-phosphate particles, and cement.

(a) Phosphate Particles. The petrographical study identified two allochemical phosphatic particles; peloids and bioclastic grains. The size of these phosphatic grains of the lower phosphorite are coarser than those in the upper phosphorites. These particles range from very coarse (up to 2 mm) in the lower phosphorite to fine (<0.2 mm) in the upper phosphorite samples. Also, the quantity of the phosphatic grains in the lower phosphorites are much higher than that of the upper one. The lower phosphorites have a closed packing texture while the texture of the upper phosphorites to be described as open packing. Optically, the phosphate minerals of the studied phosphorites occur as a cryptocrystalline and/or amorphous forms (collophane) that vary in color from brownish-yellow, grey to black as shown in Fig. 7. The variation of color from black, grey to yellow reflects the change from reducing medium of deposition to oxidizing medium of the diagenetic processes [11].

(i) Peloids. They observed as structureless, isotropic grains forming up to 55% of the phosphatic grains in the studied phosphorites. Texturally, peloids possess different shapes and sizes. Much of the studied phosphorite samples consist of coarse grained pellets up to several millimeters in diameter which made up of collophane (Fig. 7a, b). The phosphatic pellets are

rounded grains resulting of reworking of the in situ phosphate particles. The authigenic phosphatic (pristine) pellets present as isomorphous angular to subangular, oval or irregular grains (Fig. 7c). The roundness of the allochthonous phosphatic pellets may be related to the depositional hydrodynamic regime that causing strong wave activity [32]. The hydrodynamic regime was not constant even within a single stratigraphic level, as evidenced by a differently directed oblique layering. The effect of unidirectional current flow can be observed where the different phosphatic grains are oriented along one direction. The color of the pellets varies from dark yellow to pale yellow, but sometimes they have a reddish-brown color associated with ferruginous staining.

(ii) Phosphatic bioclastic grains. The studied thin sections are represented mainly by black, brownish-yellow to yellow teeth and bone fragments which are sized from medium, coarse to very coarse (up to 2 mm) grains (Fig. 7a, b, d). Teeth fragments with prismatic shape have been recorded in the studied phosphate samples in a grey to black color that occasionally stained by iron oxides red pigments (Fig. 7). Bone fragments present in the studied phosphorites in different forms and they are made up of subangular to rounded elongated forms (Fig. 7), with grey to black color which sometimes transformed into brownish red as a result of iron oxide staining. Occasionally, chalcedony replaced the apatite minerals in some bone fragments (Fig. 7b).

The reworking of the vertebrate skeletal fragments by currents can accumulate the phosphatic bioclastic grains in near shore and intertidal zones during marine transgression. The bioclasts can form

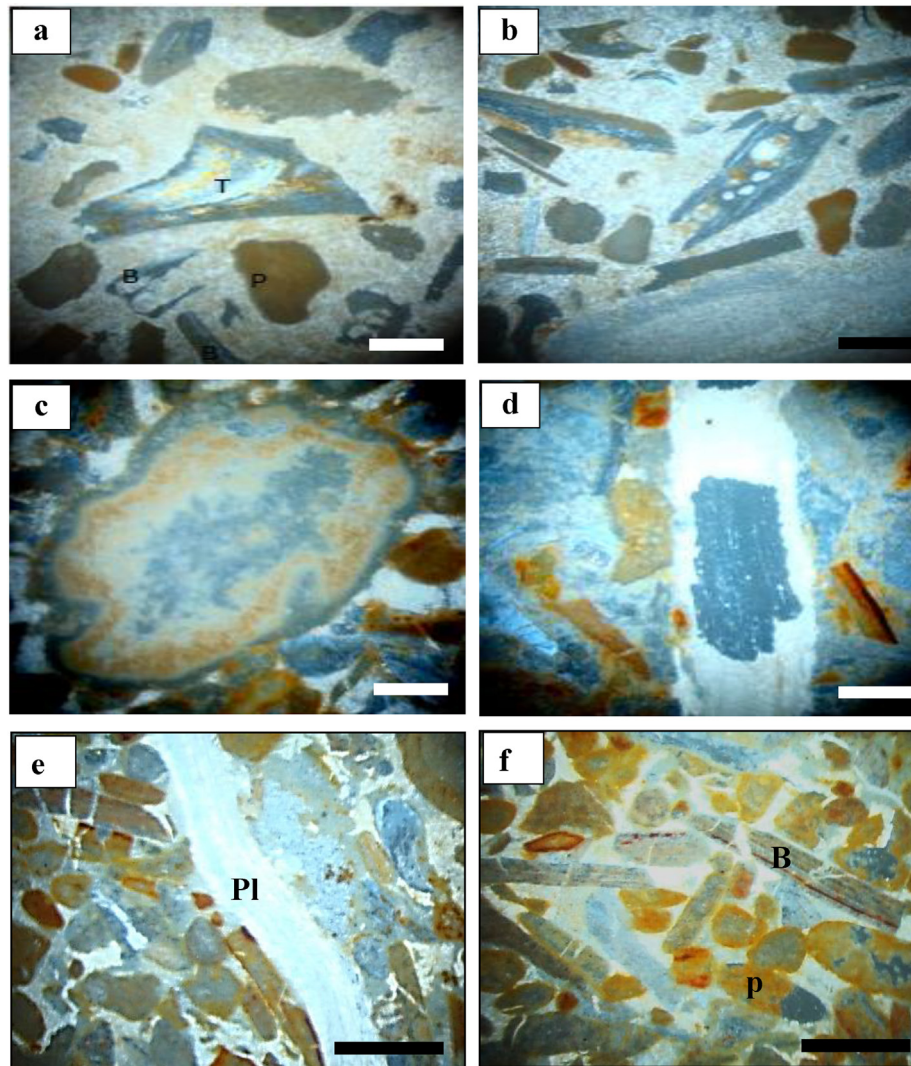


Fig. 7. Photographs showing different constituents of the studied phosphorite: a) skeletal, prismatic teeth (T), bone fragment (B) and phosphatic pellets imbedded in calcite cement; b) bioclastic phosphatic grains consisting of bone fragments embedded in amorphous silica cement; c) pristine larger phosphatic pellets and some reworked pellets; d) dissolved phosphatic grain in the central part and other dispersed phosphatic grains are stained by iron oxides; e) fine phosphatic grains and pelecypod fragments (Pl) in the upper Phosphorite Member; f) fractured bone fragments (B) and partial dissolved phosphatic pellets (P) in the Upper Phosphorite Member. Bare scale = 0.5 mm.

in association with phosphate related to upwelling process. The phosphate and phosphatized limestone fragments, as well as phosphatic fossils are very resistant to weathering agents. They are easily reworked into succeeding beds are mainly from concentrates, again of economic value [32].

(b) **Non-Phosphate Particles.** The studied phosphorite samples are represented by bioclastic pelecypod grains, detrital quartz, and rarely authigenic glauconite. The size of the pelecypod fragments reaches up to 4 mm in some phosphatic samples, especially that of the Lower Phosphorite Member. The bioclastic carbonate grains are made up of fibrous macrocrystalline

calcite, that occasionally replaced by silica. Detrital quartz is dispersed as fine – very fine, angular, spherical and longitudinal, sand grains and compose <5% of the rock.

(c) **Cementing Materials.** The examined phosphorites vary from carbonates (mainly calcite) (Fig. 7a), iron oxides, anhydrite, gypsum, to amorphous silica which represents the main partners of cement in the studied phosphorites. Silica cement presents as amorphous chalcedony mineral (Fig. 4b). Occasionally, calcite cement in the some studied phosphorite samples subjected to dolomitization and form microcrystalline dolomite.

4.2. Mineral constituents

4.2.1. Phosphate minerals

In the present study ten samples of phosphate rocks were prepared and investigated as bulk samples to determine the mineralogical composition of the studied phosphatic rocks. The most abundant and widespread minerals in the studied phosphorites are the apatite; carbonate-flour-apatite (francolite) and carbonate-hydroxyapatite (dahllite). The dahllite has been formed by the gradual crystallization of the collophane (amorphous or mineraloid calcium carbonate-phosphate) and by the migration of some of the calcium phosphate [1]. Also, the dahllite may have formed by the gradual crystallization and replacement of the collophane as well as carbonates (calcite, dolomite, few magnesite) [3]. According to [33] the francolite represents the main apatite minerals in peloids, whereas the dahllite is the substance that provides the mineral content of organically formed bones and teeth. Generally, the apatite lattice is an open lattice which allows a great number of isomorphous substitution. The XRD obtained data of the studied phosphorite samples detected the dahllite as the major phosphate mineral (Table 1). However, francolite is also present and it was difficult to distinguish between the two minerals based on their diffraction lines. The X-ray diffraction patterns of francolite and dahllite (hydroxyapatite) are similar in their general appearance and intensity distribution [34]. Also it is conformable with the general phenomenon in which a natural primary precipitate of hydroxyapatite, such as bones and teeth, pick up fluorine and changes with time in an open system toward fluorapatite composition [35]. The petrographical examination revealed enrichment of phosphatic bioclastic grains, bone and teeth fragments, in the studied phosphorites. The main characteristic reflections of francolite at 2.79, 2.69, and 1.62 Å have been detected in the pattern of all analyzed phosphate samples. Francolite and dahllite

are the main mineral constituents of west Nile Valley phosphorite [10].

4.2.2. Non-phosphate minerals

The non-phosphate minerals identified in the studied phosphorites include calcite, gypsum, quartz and dolomite (Table 1). Calcite is the major non-phosphate mineral constituent of the most studied phosphorite samples. As mentioned by petrographical studies, calcite fills the walls of bioclastic grains (pelecypod) and also presents as crystalline cements material. Occasionally, calcite has been replaced by the phosphate minerals in some bioclastic allochems. Anhydrite and gypsum are common in the studied weathered phosphate rocks and occurs as cementing material of flaky and fibrous crystals filling inter-granular pores. Presence of these sulfate minerals in the studied samples reflects the increase of sulfate (SO_4) in solution either during the deposition or during the cementation processes. Quartz is recorded in all investigated phosphorites. The petrographic examination revealed the enrichment of quartz grains and silica cement in the studied phosphorites, which conformed to the XRD results (Table 1).

4.3. Geochemical characterization

The obtained chemical analyses data of major oxides (%) of the studied phosphorite (Table 2) exhibit several proper characterizations of each sample.

4.3.1. Major oxides distribution

The Lower phosphatic member (Campanian, Upper Cretaceous), Duwi Formation, is an important rock unit resulting in relatively high enrichment of heavy metals and U content in south Esna, at the western side of the Nile Valley [3]. In the present study, three groups of major oxides distinguish the phosphorites [36] CaO , P_2O_5 , F, CO_2 , Na_2O within

Table 1. Distribution of phosphate and non-phosphate minerals in the studied phosphate rocks.

Mineral S. No.	Hydroxyl-Apatite (dahllite)	Calcite	Quartz	Gypsum	Anhydrite
17–1	✓	✓	✓		✓
28–5	✓	✓	✓		
36–10	✓	✓	✓	✓	✓
37–3	✓	✓			
32–1	✓	✓	✓		
43–4	✓	✓	✓		✓
65–7	✓	✓	✓		
73–7	✓	✓	✓		✓
83–4	✓	✓	✓		
84–8	✓	✓	✓		✓

Table 2. Chemical analyses of major oxides (%) of East Mahameid phosphorite.

Site	B.H.No.	S. No.	P ₂ O ₅	CaO	MgO	SiO ₂	Fe ₂ O ₃	F	Al ₂ O ₃	Na ₂ O	K ₂ O	L.O.I
A	17	17–1	24.1	35	5.4	13	5	2.2	1.8	1.2	0.1	10
	26	26–5	30.4	39	4	11	3	2.1	1.5	1.2	0.1	11
	27	27–3	28.5	40	2.76	10.5	3.27	1.6	1.6	1.2	0.2	10.7
	28	28–5	28.2	41.3	2.7	9.7	3	3	1.6	1.2	0.2	8
	36	36–1	30	42	7	12	5.3	2.3	1.9	1.2	0.4	14
		36–10	18	34	2.2	13	5.6	1.7	2.7	0.3	0.1	21
	37	37–1	26.4	39	3.8	10	3	0.9	1.4	1.2	0.2	11
		37–3	31	40	2.7	9	3	2.4	1.6	1.1	0.2	11
	38	38–8	30.6	42.5	2.6	9	3	3	1.4	1.2	0.1	8
	22	22–1	26.3	39.8	6	8	4	1.7	1.3	1	0.2	13
22–4		24.2	38.3	4.2	10.7	5	1.8	1.8	1.2	0.2	11	
23	23–1	27.1	38.7	6	12.8	3	1.1	2	1.2	0.3	9	
	23–4	25.2	36	4.9	10.9	4.1	2.3	1.9	1.1	0.3	10.7	
B	32	32–1	26.3	39.2	5	10.2	3	2	1.5	1.1	0.2	10.5
		32–4	23.2	35	6.9	11	4.8	1.8	1.9	1.5	0.2	13.8
	34	34–1	26.7	37	5	10	3	2.2	1.5	1.2	0.2	13.6
		34–4	24	36	5.5	13.5	5.5	2.4	2	1.6	0.2	9.6
	43	43–1	27.5	40.5	4	10.2	3	1	1.3	1	0.2	10.4
		43–4	24	38	5.3	11	4	1.0	1.9	1.2	0.1	11
	64	44–5	29	42	6.8	13	5.5	3	2	1.6	0.4	13
		64–1	24.2	37	2.8	8	2	0.7	1.3	1.1	0.1	8
	65	65–3	22.3	36	7.2	10	5	1.7	1.8	1.5	0.2	14
		65–8	30.2	42	2.2	8.6	2.8	3	1.4	1.2	0.1	7.5
73	73–8	24	35.2	5.3	12.5	5	2.2	1.8	1.2	0.1	10.5	
	74–8	22	34	7.5	12.5	5.2	1	1.8	1.6	0.2	14.2	
75	75–1	29.8	39.5	3.5	8.7	4	1.5	1.2	1.2	0.2	9.4	
	75–8	30	40	3.2	10	2.6	2.1	1.5	1.2	0.1	10.2	
83	83–4	29.7	39	2.2	9	2.4	3	1.4	1.2	0.1	8	
	84	84–5	21.8	31.3	9.5	10.4	4.3	1.4	2.5	1.1	0.2	13
		84–8	24	36	5.5	13.5	5.5	2.4	2	1.6	0.2	9.6
Min.			18	34	2.2	8	2	1	1.2	0.3	0.1	7.5
Max.			30.6	42.5	9.5	13.5	5.6	3	2.7	1.6	0.4	21
Aver.			26.1	35.77	4.8	10.7	3.9	1.9	1.7	1.19	0.19	11.35

the apatite lattice; SiO₂, Al₂O₃, K₂O, TiO₂ of the detrital origin and the Fe₂O₃, MgO, MnO of chemical weathering. The concentration of the major oxides in the studied phosphorites show similar behavior of both SiO₂, Al₂O₃, Fe₂O₃ and P₂O₅, CaO, MgO, F groups. In this respect, the unaltered francolite is mainly determined by the principal substitutions and displays only little variation of the composition of 32% P₂O₅, 52% CaO, and 4% F [37–39].

The chemical concentrations of CaO, P₂O₅, F in the studied phosphorite samples match with these of the published data of Egypt [40–43] and other worldwide localities [44] (Table 3). The P₂O₅ and cU contents in the studied phosphatic samples increase with the thickness of the Lower Phosphorite Member (Fig. 8).

Calcium oxide (42.5%) compared to that of P₂O₅ (30.6%) forming apatite recorded slight decrease. Low content of CaO and P₂O₅ were recorded within the upper member phosphorites, while SiO₂, Fe₂O₃, Al₂O₃, and L.O.I increase (Table 2). The contrast content of these oxides may be related to the

depositional conditions with minor effect of diagenetic process. Ca⁺² cation can be substituted by other elements as F (0.7–3%), in the lattice structure of apatite, and/or Mg (2.2–9.5%) by the recrystallization of calcite cement into dolomite [32]. The molecular-scale mechanisms by which substituents of varying size and charge accommodated in the apatite structure, but of fundamental importance, are poorly understood to geoscientists [45]. The decrease in CaO content is associated with increase of MgO (up to 9.5%). This behavior may be related to the diagenetic process (dolomitization) approved by the petrographical investigation that recorded microcrystalline dolomite cement.

The fluorine accumulates in phosphatic materials by the diagenetic processes. It ranges from 0.7 to 3.4% in the bones and from 1.50 to 5.48% in phosphatized coprolites [32]. Many substitutions of F in the fluorapatite structure are possible. The fluorine content increases through diagenetic processes by both the microbial action on phosphatic grains [46] and/or consolidation of phosphatic sediments [47]. Bacterial action in both coprolites and bone

Table 3. The comparison study of the studied phosphorites with other localities.

Locality Oxide (%)	1	2	3	4	5	6	7		8	
							a	b	a	b
P ₂ O ₅	26.1	25	28.27	25.95	24.75	25	23.4	28.9	32.98	30.2
CaO	38	36	40.38	39.01	38.72	39	34.21	44.4	51.76	43.6
Fe ₂ O ₃	3.9	2.23	1.63	4.00	3.38	4.3	3.09	2.02	0.231	0.79
MgO	4.79	2.54	4.33	4.68	3.4	5	0.41	1.43	0.403	0.33
F	1.72	1.74	—	1.6	1.7	3	1.37	1.53	4.04	3.2
SiO ₂	10.72	18.5	8.87	10.88	7.3	10.8	16.6	4.12	2.09	11.2
Al ₂ O ₃	1.85	6.09	2.90	1.76	1.7	1.8	4.26	0.62	0.55	1.8
Na ₂ O	1.2	0.67	1.20	1.18	0.92	1.1	0.05	0.01	n.d.	0.86
K ₂ O	0.19	0.06	0.97	0.21	0.2	0.2	0.62	0.07	n.d.	0.51
Cd	9.5	11	10	5	11	11	45	11		
Cr	114.8	128	115	58	116	128	122	92		
Cu	23.06	13	17	94	24	13	85	39		
Ni	37.4	14	34	47	36	14	50	52		
Zn	110.59	139	200	85	122	139	81	129		
Uc (ppm)	73.2	76	68	27	60	69	36,4	57.4		
Th (ppm)	3.65	3	4	5	6	3				
Ra (ppm)	69	64	69	25	65	70				

1-East El-Mahameid phosphorites (the present study).

2-El-Sibaiya East phosphorites [41].

3-Safaga-Quseir phosphorites [42].

4-El-Sibaiya West phosphorites [43].

5-Abu Tartur phosphorites [10].

6-South Esna phosphorites [44].

7 (a) Yunis mine; b) Um El-Hwuitat mine, Safaga-Quseir area [2].

8-(a) Morocco; b) Florida [45].

fragments of some Egyptian phosphorites played a great role in changing of chemical composition and elemental concentration. The bacterial tunnels have highest concentration of fluoride than other places, that due to the precipitation of fluoride by bacteria [48]. The distribution contour map of the studied phosphorites revealed the association of F, CaO and eU with the thickness of the phosphatic beds and P₂O₅ concentration (Figs. 9 and 10). In the course of phosphorite formation the fluorine content somewhat rises up during lithification of phosphorite sediments. Unconsolidated phosphate concretions - lithified phosphorite concretions shows that accumulation of fluorine in the concretions takes place somewhat in advance of phosphorus [48].

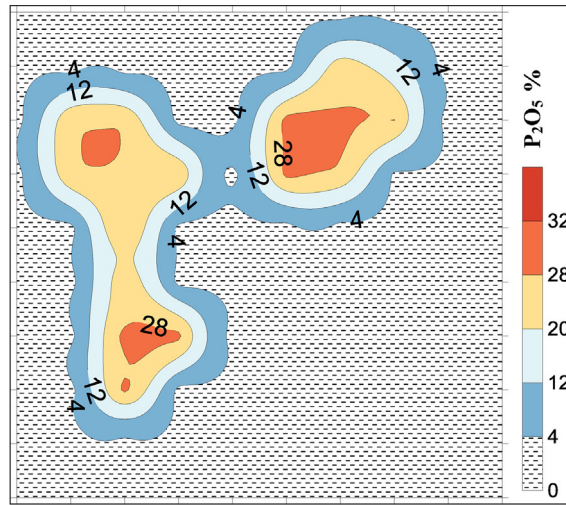
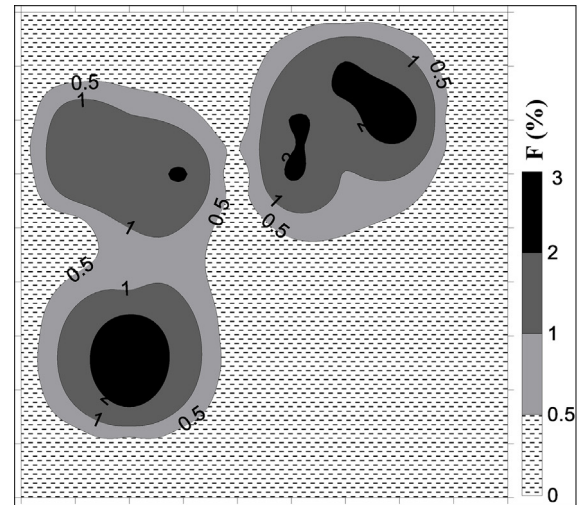
The chemical concentrations of SiO₂ (up to 13.5%) and Al₂O₃ (up to 2.7%) in the studied phosphorite samples is attributed petrographically to detrital quartz grains and/or amorphous silica in the form of chalcedony as cementing material, rather than to clay minerals (Fig. 7). In few cases the amorphous silica can be replace the phosphatic minerals in the phosphatic grins. The replacement of phosphate minerals by silica has been recorded in phosphatic rocks at Sibaiya area [48].

The studied phosphorites contain slight higher Fe₂O₃ content (5.6%) recorded as hematite and staining of the phosphatic pellets (Fig. 7). The

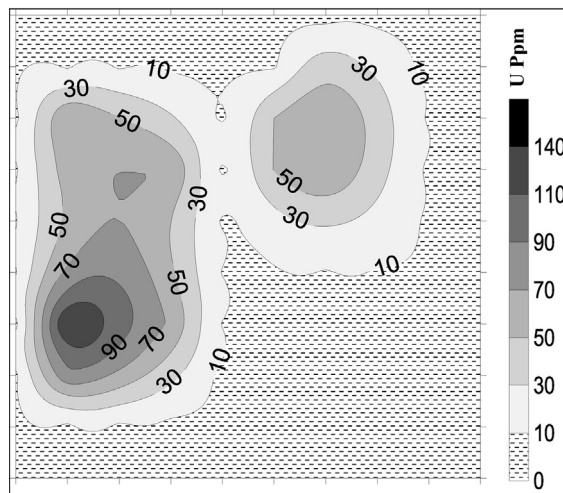
hematite mainly formed during diagenetic processes may be due to oxidation of pyrite and/or glauconite that always associate the phosphatic rocks to release Fe, S with CaO to form hematite, anhydrite/gypsum and MgO forming dolomite respectively. Anhydrite is recorded in XRD (Table 1), and hematite is detected in petrographical studies (Fig. 7).

4.3.2. Trace elements distribution

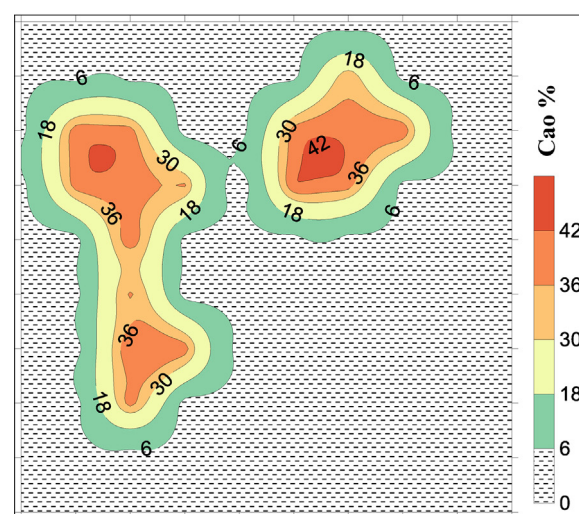
The enrichment of the trace elements in marine phosphate rocks may originate from diagenesis, hydrothermal solution or seawater [2]. The analyses of trace elements in the studied phosphorite of the Duwi Formation (Table 4) show nearly similar average contents of Cr (114 ppm) and poor Cu (23 ppm), Ni (37 ppm), Pb (4 ppm) and Zn (110 ppm) compared to marine phosphorite forgiven by [49]. Cu, Ni, Cr, and Cd contents are higher than those recorded by [31] for east and west Nile Valley. Cu and Ni in the studied phosphorites less that in phosphatic rocks south Esna that detected by [2] that can reflect different sources and depositional environment which led to the precipitation these elements in the study area. Cr is primarily carried by apatite and is further fixed in clays [50]. The elements Cu, Cr, Ni, Pb, and V show a strong affiliation to the phosphate fraction in sediments [51]. These elements are related to both replacement of the apatite lattice structure (e.g. Sr) and adsorption

(a) P₂O₅ %

(a) F (%)



(b) cU Ppm



(b) CaO %

Fig. 8. Iso-concentration maps show the concentration of P₂O₅ (a), cU (b) in the lower Phosphorite Member of the drilled Duwi Formation in East Mahameid area.

onto organic matter (e.g. Pb, Ni). Chromium, Ni, V and Pb contents are most probably adsorbed onto organic matter [52]. The concentrations of Cd, Cu, and Ni in the phosphorites may be controlled mainly mechanical weathering and climatic condition [2].

The binary relationships shown in diagrams (Fig. 11) confirm such relations. The calculated correlation coefficient (r) values of trace elements show significant confident positive correlations of CaO, Cr, Pb and U with P₂O₅, which indicates that these trace and rare earth elements are associated with phosphatic rocks. On the other hand, P₂O₅ has negative correlations with SiO₂ and Al₂O₃ which revealed that these elements may be associated with the detrital grains. Also, MgO has a negative

Fig. 9. Iso-concentration maps show the concentration of fluorine (a) and CaO (b) in the lower part of the drilled Duwi Formation at East Mahameid area.

relation with phosphorous and it may relate to diagenesis.

Strontium, Ba, and Zn exhibit a marked affinity towards fixation in the apatite crystal lattice [53]. Moreover, Sr can be concentrated in tests and shells up to 10% [54]. In this respect, Sr releases quickly from apatite crystal lattice [55] to combine with the liberated CO₃²⁻ forming strontianite beside formation of dolomite during the phosphatization diagenetic process. The field work described small dolomitic lenses that intercalated within the studied phosphorites of the lower member. All of marine carbonate fluorapatite when formed have the same Sr content (0.24%) and the recorded variations are due to later action [37].

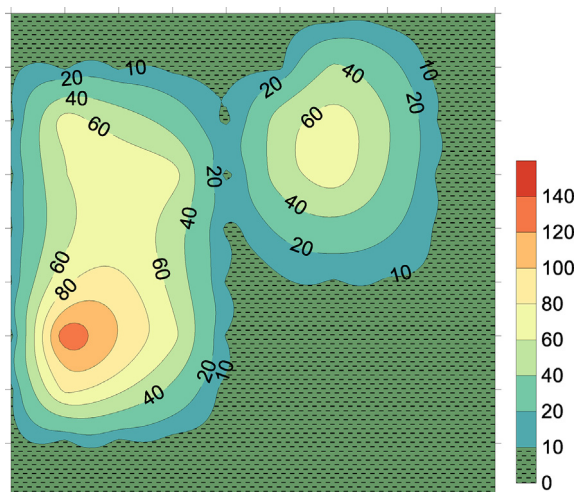


Fig. 10. Iso-concentration maps show the concentration eU (ppm) in the lower Phosphorite Member of the drilled Duwi Formation in East Mahameid area.

4.3.3. Geochemical behaviors of trace elements

The contents of the analysed trace elements (Co, Cr, Ni, Cu, Pb) show abnormal concentrations of

both Cr and Ni. Meanwhile, the radioactive element cU and eU exhibits abnormal concentrations.

The chemical Uranium (cU) iso-concentration map shows higher content in site C (up to 110 ppm) compared with site B. Moreover, the U distribution exhibits weak positive ($r = 0.17$) relation with that of P_2O_5 (Table 5). This could be attributed to post-depositional enrichment of uranium. The determined Th content is so low to be considered of valuable interest. The cU values match well with that of eU. In this respect, the iso-concentration map of each of CaO VS F as well as VS P_2O_5 exhibit similar distribution pointing to that phosphorites of the studied area characterized by presence of CaF mineral flour-apatite (Fig. 11). The plotted binary relationships between each of the major oxides VS P_2O_5 distinguished presence of negative correlation with SiO_2 and Al_2O_3 . The correlation coefficient (r) values confirmed positive correlation of correlation field (Fig. 11). However, the phosphorite sample, excluding the sample of the Upper Member. The sample of the Upper Member does not match will that the Lower Member and excluded plotted

Table 4. Concentrations of some trace and rare earth elements (REE) and radionuclides (ppm) of phosphorite of the study area.

Site	B.H.No.	S. No.	Cd	Cr	Cu	Ni	Zn	Pb	Uc	eU	Th	Ra	REEs	Uc/Th	eU/Ra	Uc/eU
A	17	17-1	11	115	28	45	205	4	50	43	6	63	283	8.3	0.68	1.16
	26	26-5	14	95	25	47	96	9	52	50	4	55	292	13	0.90	1
	27	27-3	5	129	26	41	29	3	79	70	4	74	89	19.8	0.94	1.12
	28	28-5	11	147	28	45	153	7	56	41	1	45	289	56	0.91	1.36
	36	36-1	13	138	21	39	14	3	57	51	3	64	280	19	0.79	1.1
		36-10	12	139	14	30	95	2	80	74	4	86	81	20	0.86	1
	37	37-1	22	96	32	38	64	2	75	70	4	87	95	25	0.8	1
		37-3	9	131	10	20	140	3	62	56	2	68	254	31	0.82	1.1
	38	38-8	4	135	11	12	168	2	72	68	5	73	195	14.4	0.93	1
	B	22	22-1	10	111	24	39	96	4	75	70	2	83	87	37.5	0.84
		22-4	17	85	20	41	95	7	58	51	6	63	289	9.66	0.8	1.1
23		23-1	11	82	29	46	95	1	56	51	3	62	291	18.6	0.82	1
		23-4	3	108	20	41	95	8	70	62	2	74	96	35	0.83	1.1
32		32-1	7	93	27	48	95	3	68	59	6	70	179	11.3	0.84	1.1
		32-4	11	115	28	45	205	4	90	92	6	63	283	15	1.4	0.9
34		34-1	9	117	29	45	96	11	78	70	6	85	82	13	0.82	1.1
		34-4	8	97	26	43	155	1	69	71	5	56	305	13.8	1.26	0.9
43		43-1	3	115	11	30	123	2	77	70	4	73	96	19.3	0.95	1.1
		43-4	10	113	33	41	72	3	64	66	4	59	289	16	1.11	0.9
C	64	44-5	11	111	30	47	204	6	50	45	4	62	217	12.5	0.72	1.1
		64-1	7	138	24	26	27	5	80	75	3	84	84	26.7	0.89	1
	65	65-3	7	99	27	41	153	2	65	69	4	52	285	16.3	1.32	0.9
		65-7	7	138	24	26	27	5	132	135	3	84	84	44	1.6	0.9
	73	73-8	8	155	26	42	158	4	88	90	4	53	285	22	1.69	0.9
	74	74-7	8	109	17	38	94	3	76	69	2	83	86	38	0.83	1.1
	75	75-1	13	158	19	44	181	8	74	67	2	78	192	37	0.8	1.1
		75-8	6	157	25	43	99	9	76	69	2	89	84	38	0.77	1.1
	83	83-4	8	134	24	29	57	5	112	85	3	84	82	37.3	1	1.3
	84	84-5	8	30	11	21	74	1	50	51	1	46	79	50	1.1	0.98
	84-8	6	97	26	43	155	1	69	71	5	56	305	13.8	1.26	0.97	
Min.	Min.		3	30	11	21	14	1	50	43	1	46	79	8.3	0.6	0.9
Max.	Max.		22	158	33	48	205	11	132	135	6	89	305	37.3	1.69	1.1
Aver.	Aver.		9.5	114.8	23	37.6	110.6	4.37	73.18	68.4	3.65	69	188	24.3	0.98	1.04

eU, equivalent uranium; Uc, chemical uranium.

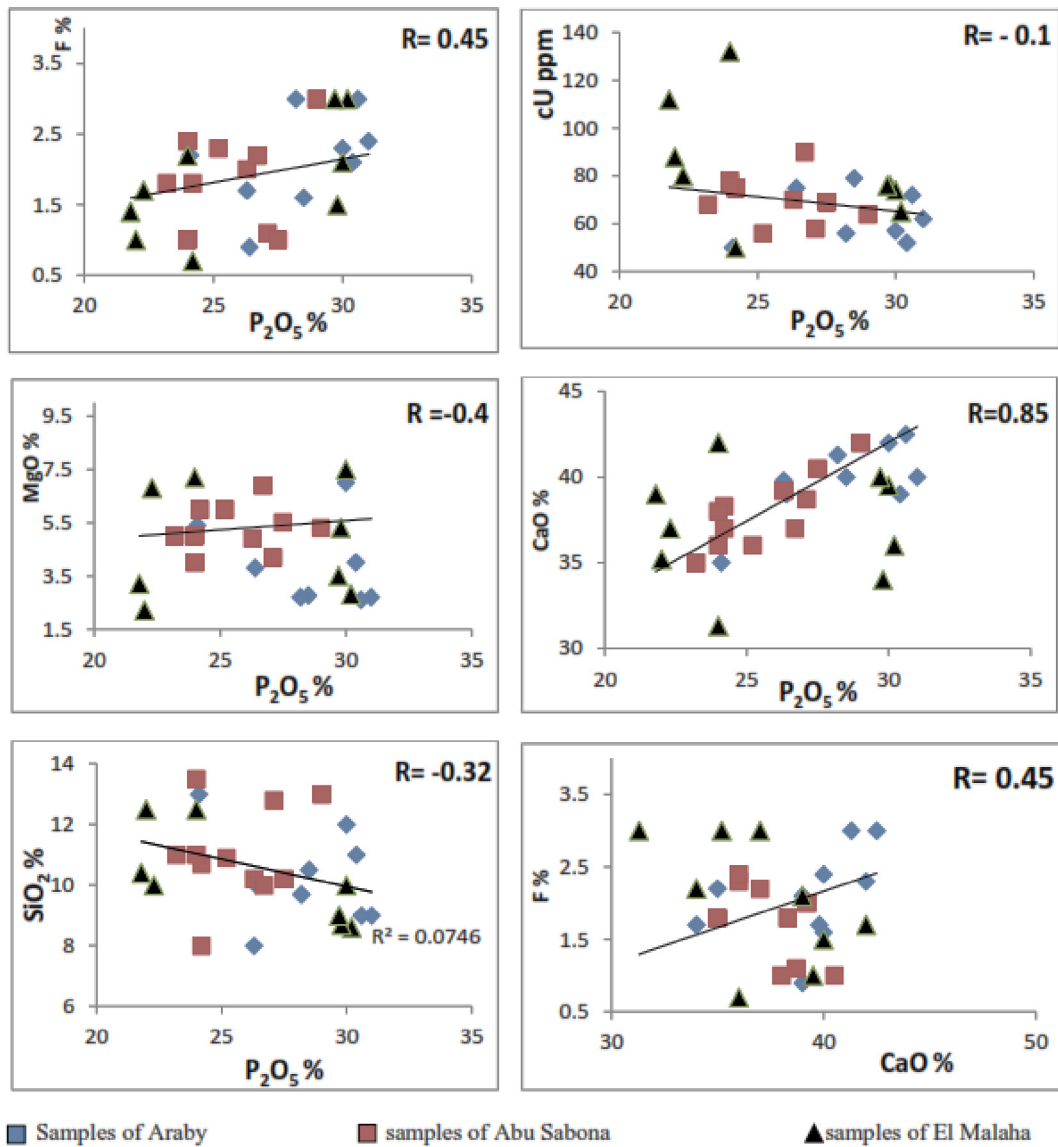


Fig. 11. Correlation between major and trace elements in the studied phosphorites of East Mahameid area.

diagrams. CaO– P₂O₅ moderate negative correlation of P₂O₅ VS each of Al₂O₃ and SiO₂. These correlations are significant and confident. The plotted F VS each of CaO and P₂O₅ shows strong.

4.3.4. Radioactive element

The radiometric cU content in the studied phosphorite ranges from 50 to 132 ppm compared to that of East Sibaiya where cU content ranges from 43 to 135 (Table 3, Fig. 8b) and that recorded in Abu Tartur phosphorite (23 ppm) [56]. Presence of U in some Nile Valley phosphorites incorporated in the apatite lattice, while the other trace elements adsorbed on clay cement [10]. It is indicated that the average of uranium, thorium and radium contents in the studied phosphorite are higher than the international averages [57–60]. The studied phosphorites could be

considered as uraniferous rocks, where they contain more than twice of Clark value (4 ppm) [61].

The Th content in the studied phosphorites ranges from 1 to 6 ppm, matching with that recorded in the other Nile Valley phosphorites (e.g. East Sibaiya phosphorite) but lower than that detected in Abu Tartur phosphorites (5 ppm) [56]. The Ra content in the studied phosphorite of East Mahameid ranges from 46 ppm to 89 ppm which is lower than that of East Sibaiya phosphorite and high Abu Tartur phosphorites.

In recent years, the radioactive equilibrium/disequilibrium study has been applied on different geological processes during Quaternary such as sedimentation in marine and continental environments [62], soil formation and evolution [63], and in dating sedimentary and volcanic rocks younger than

Table 5. Correlation coefficient values of major oxides in East Mahameid area.

	P ₂ O ₅	CaO	MgO	SiO ₂	Fe ₂ O ₃	F	Al ₂ O ₃	Na ₂ O	K ₂ O	L.O.I	Cd	Cr	Cu	Ni	Zn	Pb	Uc	eU	Th	Ra
CaO	0.85																			
MgO	-0.43	0.49																		
SiO ₂	-0.44	-0.4	0.43																	
Fe ₂ O ₃	-0.57	-0.46	0.58	0.73																
F	0.45	0.38	-0.24	0.02	0.05															
Al ₂ O ₃	-0.66	-0.61	0.47	0.71	0.68	-0.03														
Na ₂ O	0.13	0.01	0.45	0.24	0.25	0.17	-0.11													
K ₂ O	0.13	0.2	0.5	0.29	0.34	0.05	0.22	0.3												
L.O.I	-0.57	-0.43	0.36	0.35	0.56	-0.23	0.61	-0.33	0.2											
Cd	-0.04	0.04	0.04	0.09	0.15	-0.19	0.06	-0.07	0.13	0.22										
Cr	0.38	0.44	-0.63	-0.25	-0.2	0.29	-0.42	-0.19	-0.26	-0.14	-0.14									
Cu	-0.01	0.07	0.11	0.2	0.01	0.01	-0.1	0.39	0.06	-0.17	0.31	0.01								
Ni	-0.09	-0.06	0.29	0.44	0.3	-0.05	0.05	0.34	0.32	0.09	0.29	-0.05	0.73							
Zn	-0.1	-0.13	0.19	0.31	0.41	0.29	0.11	0.35	0.05	0.01	-0.02	0.05	0.03	0.25						
Pb	0.37	0.22	-0.28	-0.3	-0.29	0.26	-0.38	-0.03	-0.06	-0.12	0.11	0.35	0.19	0.34	0.01					
Uc	0.1	0.1	-0.44	-0.37	-0.3	0.16	-0.34	-0.1	-0.42	-0.18	-0.25	0.44	0.01	-0.29	-0.3	0.05				
eU	-0.02	0.01	-0.28	-0.27	-0.16	0.08	-0.22	-0.01	-0.42	-0.11	-0.25	0.33	0.03	-0.28	-0.23	-0.06	0.94			
Th	-0.2	-0.09	0.02	0.33	0.24	0.07	0.04	0.16	-0.12	0.08	0.11	-0.14	0.32	0.27	0.28	-0.07	0.01	0.06		
Ra	0.16	0.2	-0.47	-0.4	-0.39	-0.17	-0.42	-0.35	-0.21	0.08	-0.02	0.4	-0.12	-0.24	-0.4	0.24	0.56	0.42	-0.06	
REEs	0.1	0.03	0.24	0.45	0.41	0.21	0.21	0.41	0.16	-0.13	0.25	-0.09	0.29	0.4	0.51	-0.15	-0.47	-0.34	0.33	-0.77

300,000 years [64]. There are several methods and ways by which the evidences and parameters of radioactive equilibrium/disequilibrium states are estimated. These include:

- (1) Measurement of uranium content in the rocks or ores using chemical techniques, where uranium is expressed as (Uc) as well as radiometric analysis, where uranium is expressed as Ur. The equilibrium ratio (ER) is given as $ER = U_c/U_r$ [65]. The equilibrium is attained if $ER = 1$, otherwise disequilibrium is predominant.
- (2) Measurement of both the equivalent uranium (eU) and radium (Ra) concentrations (in ppm) radiometrically. The equilibrium factor (P) is given as $P = eU/Ra \cdot eU$ [66].

In the present study, the radioactive equilibrium/disequilibrium states of the investigated phosphorite deposits are discussed through the equilibrium factor (P), i.e. $P = eU/Ra \cdot eU$, and ER, i.e. $ER = U_c/U_r$. The obtained results indicate that in the equilibrium factor (P factor) in most samples is less than unity. This reflects a state of radioactive negative disequilibrium due to leaching of eU relative to Ra, eU. In contrast, in the case of ER factor in phosphorite deposits. The ER factor is higher than unity suggesting positive disequilibrium as a result of uranium enrichment in most samples (Table 3). This could be connected to recent uranium migration from the upper black shale of the Dakhla Formation to the studied phosphorite. Negative disequilibrium in ER values in the studied phosphorite may be related to uranium leaching processes by acidified water to the lowermost parts.

4.4. Conclusions

Stratigraphical evidence favored deposition of the Lower Phosphorite Member as slightly isolated lenticular bodies with maximum thickness at troughs of the epicontinental Sea. The Upper Phosphorites Member deposited in deeper seawater than the Lower Phosphorite evidenced by the small size and amount of phosphatic peloids and bioclastic grains. The similar behavior of SiO₂, Al₂O₃, Fe₂O₃ reflects the detrital origin, while P₂O₅, CaO, MgO, and F related to presence of four-apatite. The microcrystalline dolomite cement is due to a diagenetic process geochemically supported by the increase of MgO on the expense of CaO.

The abnormal concentration of Cr, Ni favor ultramafic–mafic rocks of source of the detrital material. Meanwhile the Cu contents matching with eU confirms their deposition within the phosphorite

accumulation. From the obtained results, the Lower Phosphorite Member at East Mahameid area can be recommended for local industrial production of phosphoric acid, radioactive elements and hydro-fluoric acid.

Declarations

The authors did not receive support from any organization for the submitted work.

Conflicts of interest

None.

References

- [1] Abou El-Anwar EA, Mekky HS, Abd El Rahim SH, Aita SK. Mineralogical, geochemical characteristics and origin of late cretaceous phosphorite in Duwi Formation (Geble Duwi mine), Red Sea region, Egypt. *Egypt J Petrol* 2017;26:157–69.
- [2] Abou El-Anwar EA, Mekky HS, Abdel Wahab W. P2O5– F– U characterization and depositional environment of of phosphatic rocks for the Duwi Formation, Qussier- Safaga region, Red Sea coast, Egypt. *Egypt J Chem* 2019;12:2213–28. 62.
- [3] Abou El-Anwar EA, Salman S, Mousa D, Aita S, Makled W, Gentzis T. Organic petrographic and geochemical evaluation of the black shale of the Duwi Formation, El Sebaiya, Nile Valley, Egypt. *Minerals* 2021;11:1416. 2021.
- [4] El-Kammar AM. Mineralogical and geochemical studies on El-Hagarin El-mossattaha phosphate, Sibaiya East. M. Sc. Thesis. Egypt: Cairo Univ; 1970.
- [5] Attia AM, Hulmy ME, Moursy AM. Composition and structure of phosphate deposits in A.R.E. Desert Inst Bull Cairo Egypt 1971;1:11–29. 21.
- [6] McClellan GH. Mineralogy of the carbonate fluorapatite. *J Geol Soc London* 1980;137:675–81.
- [7] Germann K, Bock WD, Schorter T. Facies development of Upper Cretaceous phosphorites in Egypt: sedimentological and geochemical aspects. *Berl Geowiss Abh A Berlin* 1984;50: 345–61.
- [8] Glenn CR, Arthur MA. Anatomy and origin of a Cretaceous phosphorite-greensand giant, Egypt. *Sedimentology* 1990;37: 123–54.
- [9] Baioumy HM. Iron-phosphorous relationship in the iron and phosphorites ores of Egypt. *Chemie der Erde Geochem* 2007; 67:229–39.
- [10] Zidan IH. Geological, mineralogical and geochemical studies of Abu-Tartur phosphate Western Desert, Egypt, PhD, Fac, Sci. Al Azhar Univ; 2002. p. 235.
- [11] Ahmad F, Farouk S, Abd El-Moghny WM. A regional stratigraphic correlation for the Upper Campanian phosphorites and associated rocks in Egypt and Jordan. *Elsevier PGA (Proc Geol Assoc)* 2014;4:419–31. 125.
- [12] National Materials Authority Report. Economic evaluation of U and REEs in Egyptian phosphorite ores. *Nucl Mater Author Rep Cairo Egypt* 2010;2:180.
- [13] Akkad S, Dardir A. Geology and phosphate deposits of Wassif, Safaga area. *Geol Survey Egypt Cairo* 1966;63:38.
- [14] Powell JH, Moh'd BK. Early diagenesis of chalk-chert-phosphorite hardgrounds (Coniacian–Campanian) of central Jordan; implications for sedimentation on a Late Cretaceous shallow pelagic ramp. *GeoArabia* 2012;17:17–38.
- [15] Cook WM, Peter J, Mc Elhinny. A re-evaluation of spatial and temporal distribution of sedimentary phosphate deposits in the light of plate tectonics. *Econ Geol* 1979;2:315–30. 74.
- [16] Cook WM, Peter J, Shergold JH. Proterozoic and cambrian phosphorites – nature and origin. In: *Phosphate deposits of the world*. Cambridge: Cambridge University Press; 1986. p. 369–86.
- [17] Abed AM. The eastern Mediterranean phosphorite giants: an interplay between tectonics and upwelling. *GeoArabi* 2013;2: 67–94. 18.
- [18] El-Naggar ZR. Stratigraphy and planktonic foraminifer of the upper cretaceous-lower-tertiary succession in the Esna-Idfu region, Nile Valley, Egypt. *Bull Nat Hist Ser Geol* 1966;2: 1–291.
- [19] Issawi B, El-Hinnawi M, Francis M, Mazhar A. The Phanerozoic geology of Egypt Ageodynamic approach. In: *Special Publication, Geological Survey Cairo*; 1999. p. 462. 76.
- [20] Ghorab MA. A summary of proposed rock stratigraphic classification for the upper Cretaceous rocks in Egypt. Read before the Geol. Soc. Egypt. April 9, 1956.
- [21] Nakkady SE. Stratigraphic study of the Mahameid district. *Bull Fac Sci Alexandria Univ* 1951;1:17–43.
- [22] Abdel Razik TM. Comparative studies on the upper cretaceous – early paleogene sediments on the Red Sea coast Nile Valley and Western Desert. Egypt, vol. 23. Algiers: The Arabian Petroleum Congress; 1972.
- [23] Kerdany MT, Cherif OH. Mesozoic. In: Said EDR, editor. *The geology of Egypt*. Rotterdam/Brookfield: Balkema; 1990. p. 407–38.
- [24] Said R. *The geology of Egypt*. Amsterdam, Oxford, New York: Elsevier; 1962. p. 259.
- [25] Youssef MM. Upper cretaceous rocks in Quseir area. *Bull Inst Desert Egypt* 1957;2:35–53.
- [26] Hassanein AM, Dardir AA, Hewaidy AA. Contribution to the stratigraphy of the upper cretaceous/Lower Tertiary succession in wasif area, Eastern Desert, Egypt. *Ann Geol Surv Egypt* 1993;19:181–206.
- [27] Awad GH, Ghorbail HG. Zonal stratigraphy of the Kharga Oasis. *Geol Surv Egypt* 1965;34:75.
- [28] Hermina MH. Geology of the north western approaches of Kharga. *Geol Surv Egypt* 1967;44:88.
- [29] Issawi B, Hassan Y, Saad A. Geology of the Abu Tartur plateau, Western Desert, Egypt. *Geol Surv Ann* 1978; 8:91–127.
- [30] Youssef MI. Genesis of bedded phosphates. *Econ Geol* 1965; 60:590–600.
- [31] El-Kammar A, El-Kammar M. On the trace elements composition of the Egyptian phosphorites: a new approach. In: *6th international conference on the geology of the Arab world*. Cairo: Cairo University; 2002. p. 227–44.
- [32] Trappe J. Phanerozoic phosphorite depositional systems. A dynamic model for sedimentary resource system. *Lect Notes Earth Sci* 1998;76:316.
- [33] Heinrich EW. *Microscopic petrography*. New York, Toronto, London: Mc Graw Hill Book Co; 1956. p. 296.
- [34] Bhatnagar VM. Infrared spectra of hydroxyapatite and fluorapatite. *Bulletin de la Societe Chimique de France* 1968; 91(1):1771–3.
- [35] Gulbrandsen RA. Chemical composition of phosphorites of the phosphoria formation. *Geochem Cosmochim Acta* 1966; 30:365–82.
- [36] Cook PJ. Petrology and geochemistry of the phosphorite deposits of north west Queensland, Australia. *Econ Geol* 1972;67:1193–213.
- [37] McArthur JM. Systematic variations in contents of Na, Sr, CO₃ and SO₄ in marine carbonate-fluorapatite and their relation to weathering. *Chem Geol* 1978;1–2:89–112. 21.
- [38] McArthur JM. Francolite geochemistry-compositional controls during formation, diagenesis, metamorphism and weathering. *Geochem Cosmochim Acta* 1985;1:23–35. 49.
- [39] Jarvis NJ, Stahli M, Bergstrom LF, Johnson H. Simulation of dichlorprop and bentazon leaching in soils of contrasting texture using the MACRO model. *J Environ Sci Health* 1994; 29:1255–77.
- [40] Jarvis NJ, Stahli M, Bergstrom LF, Johnson H. Simulation of dichlorprop and bentazon leaching in soils of contrasting texture using the MACRO model. *J Environ Sci Health* 1994; 29:1255–77.

- [41] Negm SH. Mineralogical and geochemical studies on the phosphorite of El-Sibaiya area, Nile Valley, Egypt. M.Sc. Thesis. Minufia University; 2009.
- [42] Hebeish AA. Mineralogical and geochemical studies of the phosphate deposits of the Red Sea coast, eastern Desert, Egypt. Cairo, Egypt. Department of Geology, Faculty of Science, Al-Azhar Univ; 2008.
- [43] Hassaan MM, Zidan IH, Mohamed WA, Hatem E, Elshazly MM. Uranium bearing phosphorite, West Sibaiya, Egypt: exploited mines characterization and potential of surrounding areas. *Curr Sci Int* 2017;6:377–95.
- [44] Zidan IH. Evaluation of phosphorite and uranium in lower member, Duwi Formation at Kummer area south Esna, west Nile valley, Egypt. *J Sedimentol Soc Egypt* 2013;21:143–54.
- [45] Potts PJ, Tindle AG, Webb PC. Geochemical reference material composition, F1. Boca Raton: CRC Press; 1992.
- [46] Vaughn JS, Lindsley DH, Nekvasil H, Hughes JM, Phillips BL. Complex F,Cl apatite solid solution investigated using multinuclear solid-state NMR methods. *J Phys Chem C* 2017;30:30p.
- [47] Boggs JR. Petrology of sedimentary rocks. 2nd ed. Cambridge UK: Cambridge University Press; 2009. p. 600.
- [48] Batturin GN. Phosphorites on the Sea floor-origin, composition and distribution. Amsterdam: Elsevier; 1982.
- [49] Abdel Moghny WM. Lithology of the phosphatic rocks of Duwi Formation, Egypt. Ph.D. thesis. Voronezh State University; 2011. p. 154.
- [50] Altschuler ZS. The geochemistry of trace elements in marine phosphorites. Part I: characteristic abundances and enrichment. *SEPM Spec Pub* 1980;29:19–30.
- [51] Privot L, Lucas J. Behavior of some trace elements in phosphatic sedimentary formations. *Soc Econ Paleont Min Spec Pub* 1980;29:31–9.
- [52] Jarvis I. Sedimentology, geochemistry and origin of phosphatic chalks, the Upper Cretaceous deposits of NW Europe. *Sedimentology* 1992;39:55–97.
- [53] El-Kammar AM. Comparative mineralogical and geochemical study on some Egyptian phosphorites from Nile Valley, Quseir area and Kharaga Oasis. Ph. D. Thesis. Egypt: Cairo Univ; 1974.
- [54] Altschuler ZS. The geochemistry of trace elements in marine phosphorites, Part I Characteristic abundance and enrichment. *Soc Econ Paleont Min Spec Pub* 1980;29:19–30.
- [55] Kulp JL, Turkein K, Boyd DW. Strontium content of limestone and fossils. *Geol Soc Am Bull* 1952;63:701–16.
- [56] Lucas J, Flicoteaux R, Nathan Y, Prevot L, Sahar Y. Different aspects of phosphorite weathering. In: *Marine phosphorites*. SEPM, Special Publications. 29; 1980. p. 41–51.
- [57] UNSCEAR. United Nations Scientific Committee on the effects of atomic radiation, sources and effects of ionizing radiation. In: Report to general assembly, with scientific annexes United Nations. New York: United Nations; 2000. p. 654.
- [58] International IAEA. Atomic energy agency ‘Gamma-ray Survey in uranium exploration. In: IAEA technical report series. vol. 186; 1979. p. 90.
- [59] Boyle RW. Geochemical prospecting for thorium and uranium deposits. Amsterdam: Elsevier Publications Co; 1982. p. 498.
- [60] EL-Kammar AM, EL-Feky MG, Abu zied HT, Othman DA. Radioactivity and environmental impacts of some Carboniferous and Cretaceous kaolin deposits in Southwestern-Sinai, Egypt. *Nucl Sci Scient J* 2018;7:87–100.
- [61] Clark S, Peterman J, Heier K. Abundance of uranium, thorium and potassium. In: Clark SP, editor. Handbook of physical contents, vol. 24. Memoir of the Geological Society of America; 1966. p. 521–41. 97.
- [62] Burnett WC, Veeh HH. Uranium-series studies of marine phosphates and carbonates. In: Ivanovich M, Harmon RS, editors. Uranium series disequilibrium: applications to Earth, marine and environmental Sciences. 2nd ed. Oxford: Science Publications, Oxford University Press; 1992. p. 487–512.
- [63] Mathieu D, Bernat M, Nahon D. Short-lived U and Th isotope distribution in a tropical laterite derived from granite (Pitinga river basin, Amazonia, Brazil): application to assessment of weathering rate. *Earth Planet. Sci Lett* 1995; 136:703–14.
- [64] Ivanovich M, Latham AG, Ku L. Uranium series disequilibrium applications in geochronology. In: Ivanovich M, Harmon RS, editors. Uranium series disequilibrium: applications to Earth, marine and environmental sciences. 2nd ed. Oxford: Science Publications, Oxford University Press; 1992. p. 62–85.
- [65] El Feky M, Mohammed H, El-Shabasy A, Ahmed M, Abdel-Monem Y, Mira H. Mobilization of radionuclides during uranium and gold processing of granitic rock at El-Missikat area, central Eastern Desert, Egypt. *Int J Environ Anal Chem* 2021, in press. <https://doi.org/10.1080/03067319.2021.1925262>.
- [66] El Galy MM, El Mezayn AM, Said AF, El Mowafy AA, Mohamed MS. Distribution and environmental impacts of some radionuclides in sedimentary rocks at Wadi Naseib area, southwest Sinai, Egypt. *J Environ Radioact* 2008;99: 1075–82.